International Journal of Modern Physics E, Vol. 10, No. 3 (2001) 185–208

DISCOVERY OF LONG-LIVED SHAPE ISOMERIC STATES WHICH DECAY BY STRONGLY RETARDED HIGH-ENERGY PARTICLE RADIOACTIVITY

A. MARINOV and S. GELBERG
Racah Institute of Physics, The Hebrew University, Jerusalem 91904, Israel

D. KOLB
Department of Physics, Kassel University, 34109 Kassel, Germany

Received 29 May 2001

The reaction ^{28}Si + ^{181}Ta has been studied at $E_{\rm Lab} = 125$ and 135 MeV. Coincidences between high energy particles from abnormally long-lived states and various X- and γ-rays were observed, e.g. 7.8–8.6 MeV α-particles with γ-rays of a superdeformed band, 5.1–5.5 MeV α-particles with X- and γ-rays of W, Re and Pt, and 3.88 MeV particles (interpreted as protons) with 185.8 keV γ-rays. The data are interpreted in terms of the production of long-lived ($t_{1/2}$ of several months) high spin isomeric states in the second well of the potential in the parent nuclei, which decay to the normal states in the daughters, and in the third well of the potential, which decay to the second well.

1. Introduction

The first evidence for a new kind of long-lived isomeric state was obtained in actinide fractions[14,2] produced via secondary reactions in a CERN W target which had been irradiated with 24 GeV protons.[3] Isomeric states with $t_{1/2} \sim 0.6$ y and ≥ 30 d (10^4–10^5 times longer than the expected half-lives of the corresponding ground states) were found in neutron-deficient ^{236}Am and ^{236}Bk nuclei, respectively. About 3×10^5 atoms of ^{236}Am and 4×10^4 atoms of ^{236}Bk were produced in the isomeric states, and decayed by the β^+ or electron capture processes. The character of these states was not clear; they are far from closed shells where high spin isomers are usually found, and they have very long lifetimes as compared to the known shape isomers.

In addition,[2,4,5] some new particle groups were found in the decay of various actinide fractions separated from the same W target. For example, an unambiguous 5.14 MeV α-particle group with $t_{1/2} \sim 4$ y was seen in the Bk source.[1,2,4–6] This half-life is a factor of 2×10^6 to 3×10^3 too short as compared to the deduced half-life from energy–lifetime relationship[7] for normal α-decay of such energy from Bk–Pu nuclei. It was very difficult to understand such an enhancement. Furthermore, 3.0 and 4.0 MeV particle groups from the Am source were seen in coincidence with $L_{\alpha1}$ X-rays in the Am region.[2] Since the relationship between the particle energies

and their lifetimes deviates by about 23 and 12 orders[4] from the systematics[7] of α-particles, it was assumed[4] that they were protons of unknown origin.

The clue to the understanding of the above mentioned findings has been obtained recently in several studies[8,9] of the $^{16}O+^{197}Au$ reaction at $E_{Lab} = 80$ MeV, where similar isomeric states and particle decays were found. An isomeric state which decays by emitting a 5.20 MeV α-particle with $t_{1/2} \sim 90$ mn has been found in ^{210}Fr. Since this half-life is longer than the known half-life of the ground state of ^{210}Fr, it was concluded that a long-lived isomeric state had been formed in this nucleus. A $t_{1/2}$ of 90 mn for 5.20 MeV α-particles in ^{210}Fr is enhanced by a factor of 3×10^5 as compared to normal transitions.[7,8] However, this group was observed in coincidence with γ-rays which fit predictions for a super-deformed band.[8] Therefore the effect of large deformations of the nucleus on the α-particle decay was calculated and found[8] to be consistent with the observed enhancement. It was argued[8] that since the isomeric state decays to a high spin state, it should also have high spin, and since it decays by enhanced α-particle emission to state(s) in the second well of the potential, it should be in the second well itself.

The predicted[10,11] excitation energies of the second minima in the evaporation residue nuclei and their daughters produced by the $^{16}O + ^{197}Au$ reaction are above the proton separation energies. Therefore a search for long-lived proton decays has been performed[9] using the same reaction. Two long-lived proton activities with half-lives of about 6 h and 70 h were found[9] with proton energies of 1.5–4.8 MeV with a sharp line at 2.19 MeV. This energy may correspond to a predicted transition[10] from the second minimum in ^{198}Tl to the ground state of ^{197}Hg with $E_p = 2.15$ MeV. The superdeformed state in ^{198}Tl may be produced in an alpha decay chain of transitions from shape isomeric states to shape isomeric states starting from ^{210}Fr. It should be noted that a long-lived high-spin isomeric state in the second minimum of the potential in ^{241}Pu was predicted by S. G. Nilsson *et al.*[12] back in 1969.

The present work reports on the discovery of new long-lived isomeric states, produced by the $^{28}Si + ^{181}Ta$ reaction at bombarding energies of 125 and 135 MeV, which decay by strongly hindered α-particle and proton transitions. The lower energy is about 10% below the Coulomb barrier. A fusion cross section of about 10 mb is predicted for this energy using a coupled-channel deformation code[13] with deformation parameters $\beta_2 = 0.41$ for ^{28}Si and $\beta_2 = 0.26$ for ^{181}Ta,[14a] and allowing for 2^+ and 3^- excitations in ^{28}Si. Only 2 μb is predicted when no deformations are included in the calculations. For 135 MeV the corresponding predicted fusion cross sections are 95 mb with deformations and 40 mb without. At bombarding energies of 125 and 135 MeV, the compound nucleus is formed at excitation energies of 42.1 and 50.8 MeV, respectively. Preliminary results of this work have been published before.[6,15–17]

[a]The β_2 value for ^{181}Ta was taken as the average from the corresponding values of ^{180}Hf and ^{182}W.

2. Experimental Procedure

In three irradiations, 2.5 mg/cm^2 Ta targets followed by stacks of C catcher foils were bombarded with a ^{28}Si beam obtained from the Pelletron accelerator in Rehovot. Irradiations I and II were performed with a 125 MeV ^{28}Si beam and irradiation III with 135 MeV. Carbon catcher foils of 200 μg/cm^2 and 60 μg/cm^2 were used in order to catch the evaporation residue nuclei and their daughters. In all experiments the average beam intensity was about 11 particle-nA and the total dose about 1×10^{16} particles. Long period off-line measurements were carried out in the laboratory in Jerusalem, using the irradiated catcher foils as sources. In the present paper we summarize the results of the particle-γ coincidence measurements.[b] A 450 mm^2, 300 μm thick, Si surface barrier detector and a 500 mm^2, 10 mm thick, thin window Ge(Li) detector were used for these measurements. The Si detector was calibrated using the 3.18 MeV α-particle group of a ^{148}Gd source and an accurate pulse generator. The Ge(Li) detector was calibrated using the X- and γ-rays of a ^{57}Co source. The source was sandwiched between the Si and the Ge detector. Two 0.01 inch thick Be foils separated the source from the Ge detector. The first foil was the window for the vacuum chamber which included the source and the Si detector, and the second one the window of the Ge detector. The transparency of the two Be windows together was close to 100% for gamma-rays with $E_\gamma \geq 10$ keV. The solid angle of the Si detector was about 34% of 4π sr and of the Ge(Li) detector 16%. The peak-to-total ratio of the Ge(Li) detector was 100% up to about 120 keV and decreased gradually to 22% at 250 keV. Its FWHM energy resolution was about 900 eV. The intrinsic resolution of the Si detector was about 25 keV. The full line widths for α-particles of 5.0–8.6 MeV were 0.5–0.34 MeV, respectively, with a 200 μg/cm^2 C foil, and the corresponding values for the 60 μg/cm^2 foil were 0.16–0.10 MeV. The resolving time of the coincidence system was set electronically to 1 μs and was checked by using a strong γ-ray source from one side and a random pulse generator from the other side, using the well known relationship $N_R = 2\Delta N_1 N_2$. In this formula Δ is the resolving time, N_R is the random coincidence intensity and N_1 and N_2 are the singles intensities from both sides. The coincidence events together with the singles particle events were recorded event by event with a time accuracy of 1 ms.

It is worthwhile mentioning that because of the compact geometry the solid angle of the single small Ge detector used by us was about twice as large as of that of the current big γ-ray arrays. For coincidences between for instance three γ-rays (which will appear as sum events in the single detector, see Sec. 3.2 below), the ratio of the effective solid angles increases by a factor of about eight. The long

[b] α–α correlation measurements were performed with 60 μg/cm^2 C catcher foils situated in between two 300 μg/cm^2 Si detectors, but no α correlation events with $\Delta t \leq 10$ s could be significantly established. The preliminarily claimed correlations[15] cannot presently be ruled out as due to other physical or electronic background effects. At longer correlation times the number of random events was too large.

period of the off-line measurements of 77 to 235 days, which is required when one searches for the production of long-lived new radioactivity, adds another advantage to the present experimental procedure which is not easy to achieve otherwise.

3. Results

3.1. *Singles and coincident events*

Figures 1 and 2 show typical singles particle and γ-ray spectra obtained at 125 MeV bombarding energy. Figures 3 and 4 show similar spectra obtained at 135 MeV beam energy. From the measured α-particle and γ-ray energies and lifetimes, production cross sections for various evaporation residue nuclei, with estimated errors of $\pm 25\%$, were deduced and are summarized in Table 1. (Cross sections for some isomeric states — see below — are also given in Table 1.)

Figures 5 and 6 give respective α–γ coincidence plots from measurements I and II, corresponding to irradiations I and II. Figures 7 and 8 are one-dimensional projection plots on the α-particle axis of Figs. 5 and 6, respectively, for $E\gamma \geq 25$ keV. Figure 9 presents a particle–γ coincidence spectrum from measurement III, corresponding to irradiation III.[c] The estimated numbers of random coincidences in the 3–10 MeV particle energy and 10–250 keV γ-energy are 5.4×10^{-2}, 4.4×10^{-2}, and 0.4 in Figs. 5, 6, and 9, respectively. Some of the coincidence events in Figs. 5, 6 and 9, between 5–6 MeV α-particles and various γ-rays, may perhaps be due to a contamination from an emanated ^{212}Pb source from ^{228}Th, which was used in the same chamber about 4 months earlier.[9] Despite the long delay time to our present long term measurements of 77 to 235 days, and careful cleaning of the chamber, we might have picked up some residual contamination. Also, indication for K X-rays of Rn is seen in this region. While in principle their origin may be from some reaction products, they also may be from the decay of ^{223}Ra, which belongs to the ^{235}U chain. Although it is not likely, but because of this ambiguity, we will not try to make a claim about this region. A two-dimensional background measurement, taken for 8 days, before the ^{212}Pb source was used in the chamber, gave zero events in the whole region of 3.5–10 MeV particles and 0–250 keV γ's.

It is seen in Figs. 5 and 6, and Figs. 7 and 8, that while the region of α-particles of 6–8 MeV is relatively empty, coincidence events are seen between various γ-rays and α-particles of 8–9 MeV. In Fig. 5, 13 coincidence events between 7.99–8.61 MeV α-particles and various γ-rays of $E \geq 20$ keV are observed, where 8 of them fall within a narrow range of 190 keV particle energy, between 8.42–8.61 MeV. (The estimated α-particle full line width for the 200 μg/cm^2 C foil is around 340 keV.)

[c]During the first 77 d after irradiation I was completed, a search for proton activity using the ΔE–E system of Ref. 9 was performed and gave negative results with an upper limit of about 0.5 nb for half-lives of between 20 hours to 70 days. On the other hand, in the 135 MeV experiment (Fig. 9) we most probably saw protons in the particle–γ coincidences. (See Sec. 3.4).

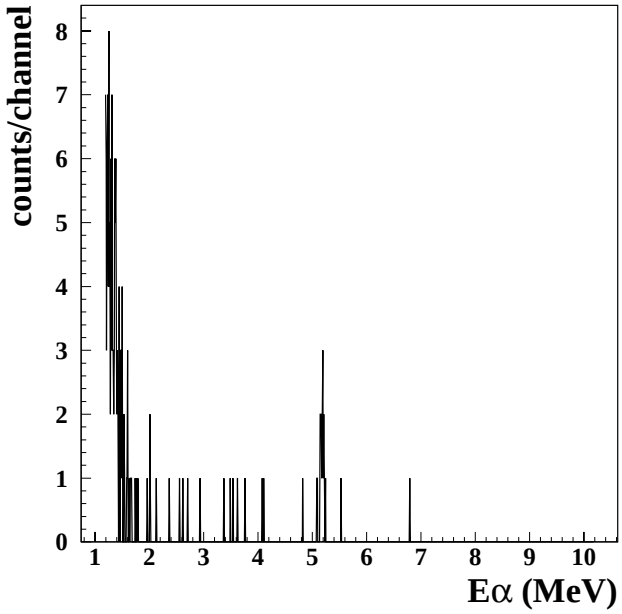

Fig. 1. Typical particle singles spectrum at $E_{\mathrm{Lab}}(^{28}\mathrm{Si}) = 125$ MeV with a 60 μg/cm^2 C catcher foil, taken for 29 hours starting three hours after the end of irradiation.

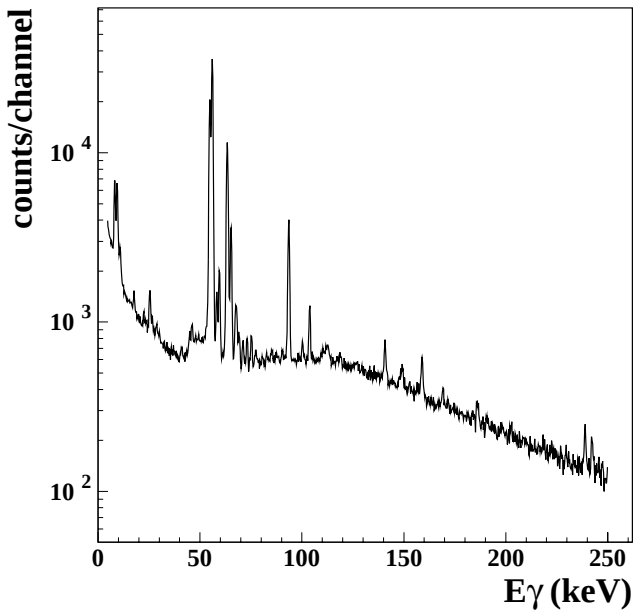

Fig. 2. Typical γ-ray singles spectrum. Same conditions as Fig. 1.

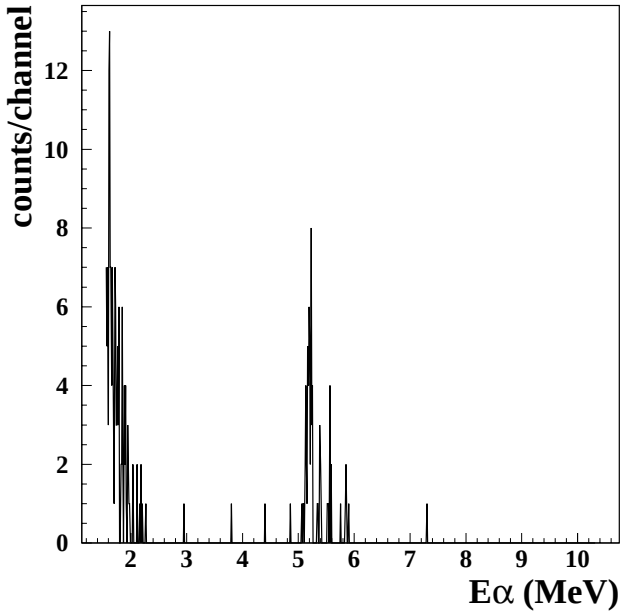

Fig. 3. Typical particle singles spectrum at $E_{\rm Lab}(^{28}{\rm Si}) = 135$ MeV with a 60 μg/cm^2 C catcher foil, taken for 11 hours starting three hours after the end of irradiation.

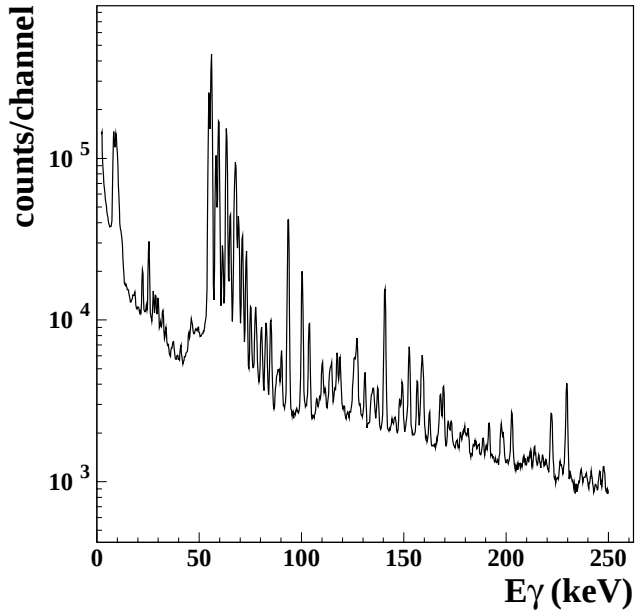

Fig. 4. Typical γ-ray singles spectrum at $E_{\rm Lab}(^{28}{\rm Si}) = 135$ MeV with a 200 μg/cm^2 C catcher foil, taken for 24.5 hours, starting three hours after the end of irradiation.

Table 1. Production cross sections for various evaporation residue nuclei obtained in their ground states and in the isomeric states via the ^{28}Si + ^{181}Ta reaction at 125 and 135 MeV.

Reaction	$\sigma^{\text{g.s.}}$ (μb) 125 MeV	$\boldsymbol{\sigma^{\text{i.s.}}}$ **(nb) 125 MeV**	$\sigma^{\text{g.s.}}$ (μb) 135 MeV	$\boldsymbol{\sigma^{\text{i.s.}}}$ **(nb) 135 MeV**
3n	≤ 3.4	$\geq$ **8**[a]	≤ 155[b]	
p2n	4.5		≤ 23[b]	
4n			274	$\leq$ **9**[d]
p3n			101	$\geq$ **3**[a]
5n			≤ 21[c]	
p4n			≤ 21[c]	
α2n				$\geq$ **2**[a]
pn		$\geq$ **12**[a,e]		

[a]A lower limit is given since the branching ratios along the decay chain (Table 3) are not known.
[b]It was impossible to distinguish between the 3n and the p2n reactions. The value given was deduced assuming that the relevant observed activity is due to this reaction channel only.
[c]It was impossible to distinguish between the 5n and the p4n reactions. The value given was deduced assuming that the relevant observed activity is due to this reaction channel only.
[d]Based on the coincidence group of the 3.88 MeV protons with 185.8 keV γ-rays and assuming that the γ-rays are from ^{204}Rn (see Sec. 3.4 and 4.3).
[e]This value is obtained assuming that the 8.6 MeV α's decay to a 39/2 state. About a factor of two lower value is obtained if 25/2 is the maximum spin of the produced SDB and larger cross sections correspond to larger maximum produced spin values (see Sec. 3.2).

From the intensities of the singles in the α- and γ-ray spectra (339 α-particles and 2.14×10^7 gamma-rays in 76.8 days), and the resolving time of 1 μs of the coincidence system, the total number of random coincidences in the 8–9 MeV region was estimated to be 2.2×10^{-3}. In Fig. 6 one finds 8 coincidence events between 8.19–9.01 MeV, where 5 of them fall within 70 keV, between 8.55–8.62 MeV, and one at 9.01 MeV. (The α-particle full line width for a 60 μg/cm^2 C foil is about 100 keV.) The corresponding estimated total number of random coincidences between 8 and 9 MeV is 1.4×10^{-3}. One does not see such concentration of events in the same energy region in Fig. 9 which was taken for about 2.7 times longer period than Figs. 5 and 6. Three events are seen in the 8–9 MeV region in Fig. 9 which sets an upper limit on the background in Figs. 5 and 6 to be around one count as compared to the respective 13 and 8 counts seen experimentally. It was estimated that in the 8–9 MeV range of α-particles, at most 0.8 events in Fig. 5 and 0.3 events in Fig. 6 may be due to the contamination mentioned above of coincidences between β^- and γ-rays from ^{212}Bi and the 8.78 MeV α-particles from ^{212}Po ($t_{1/2} = 0.3$ μs).

It should also be mentioned that in three cases (see comments "c", "d" and "e" in Table 2) two events appeared at the same position within the energy resolution.

Figure 10 shows time sequence plots for the α–γ coincidences with α-energies of 8–9 MeV obtained in measurements I and II and seen in Figs. 5 and 6, respectively.

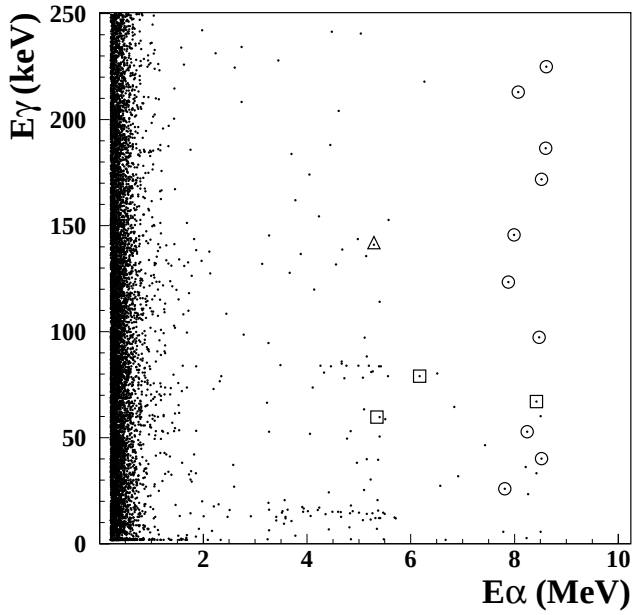

Fig. 5. Particle-γ coincidences from measurement I: $E_{\rm Lab}(^{28}{\rm Si}) = 125$ MeV, with a 200 μg/cm^2 C catcher foil, taken for 76.8 days, starting 77.4 days after the end of irradiation. The γ-ray energies of the encircled events fit with SDB transitions. The photon energies of the events in squares fit with known characteristic X-rays. The γ-ray energies of the events in triangles are identified with known transitions.

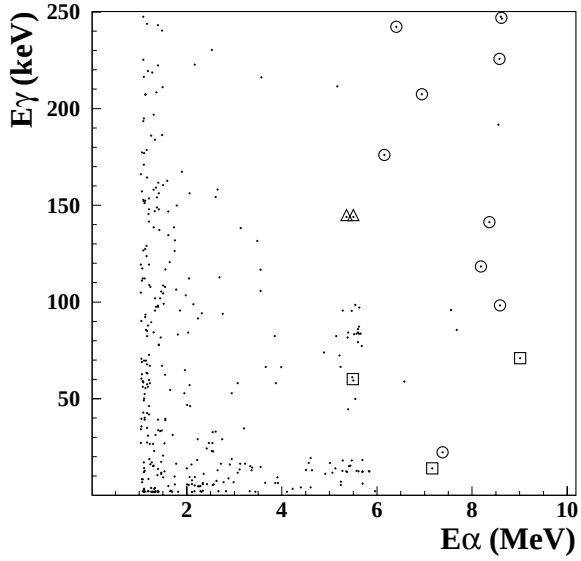

Fig. 6. Particle-γ coincidences from measurement II: $E_{\rm Lab}(^{28}{\rm Si}) = 125$ MeV, with a 60 μg/cm^2 C catcher foil, taken for 96.7 days, starting three hours after the end of irradiation. For further explanations see Fig. 5.

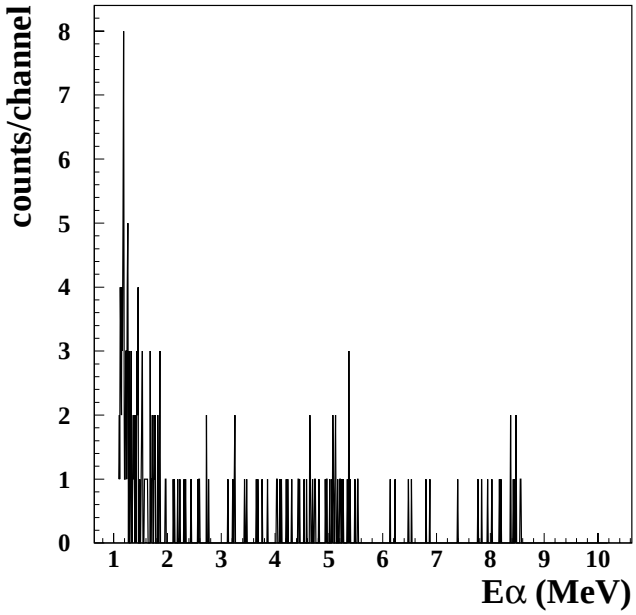

Fig. 7. Projection of the α–γ coincidence events seen in Fig. 5 on the α-particle axis for $E_\gamma \geq$ 25 keV.

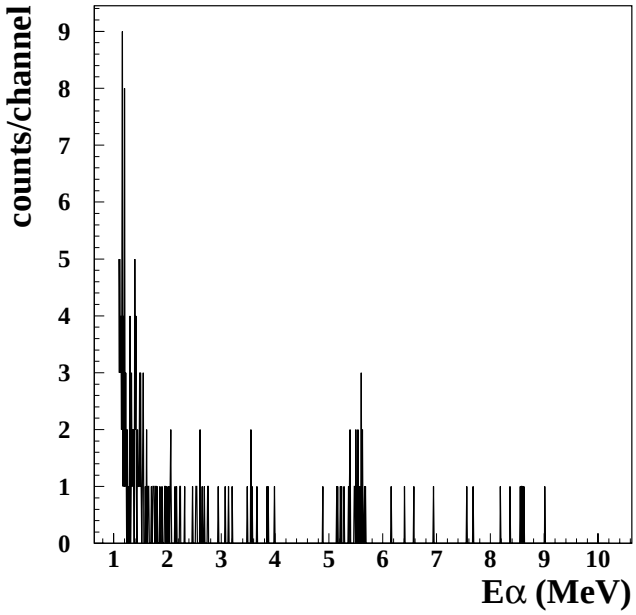

Fig. 8. Projection of the α–γ coincidence events seen in Fig. 6 on the α-particle axis for $E_\gamma \geq$ 25 keV.

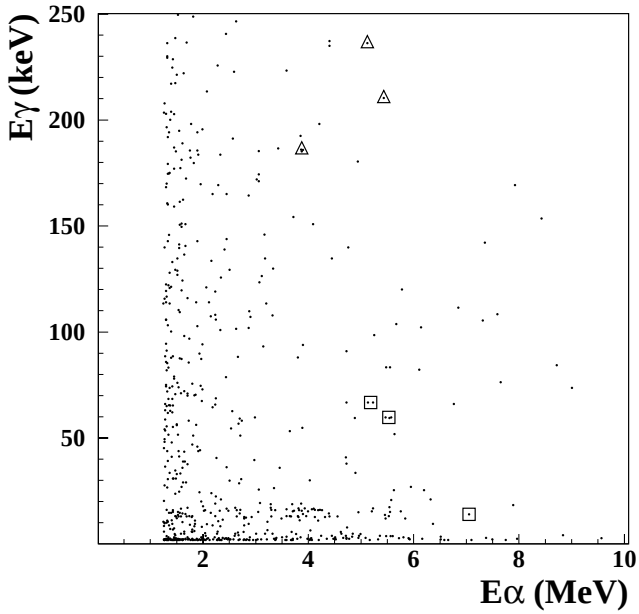

Fig. 9. Particle-γ coincidences from measurement III: $E_{\rm Lab}(^{28}{\rm Si}) = 135$ MeV, with a 200 μg/cm^2 C catcher foil, taken for 235 days, starting three hours after the end of irradiation. For further explanations see Fig. 5.

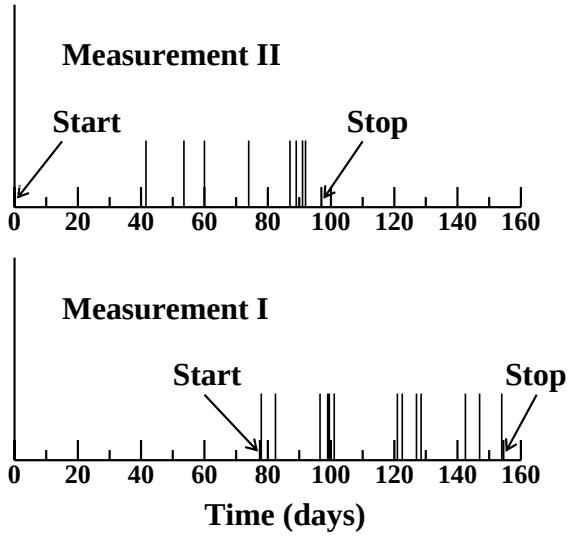

Fig. 10. Time sequence plots for the α–γ coincidences with 8–9 MeV α-particles obtained in measurements I and II and seen in Figs. 5 and 6, respectively.

In measurement II, a growth in the intensity of the 8–9 MeV group was found from the beginning up to 97 days after the end of irradiation. In measurement I, no significant change in decay rate was observed between 77 and 154 days and, by binning the data, $t_{1/2} \geq 40$ days was estimated for the lower limit of the decaying half-life. An additional measurement, taken about 4.5 y after the one presented in Fig. 5 and measurement I of Fig. 10, gave zero counts in 22.0 d. An upper limit for the half-life of $t_{1/2} \leq 2.1$ y is deduced from this measurement.

3.2. *Rotational bands and sum events*

Table 2(a) and Fig. 11 show that almost all the coincidence events in Figs. 5 and 6 with 7.8–8.61 MeV α-particles (the circled ones) fit very nicely with a $J(J+1)$ law assuming $E_x = 4.42 \times J(J+1)$ keV and $\Delta J = 1$. This fit is very significant from a statistical point of view.[8] All the gamma-rays in Fig. 5 (7 out of 7 events), and almost all of them in Fig. 6 (6 out of 7 events), which are above 90 keV, fit on average to within ± 0.5 keV, with this formula. The probability for 13 out of 14 events which are distributed evenly (for instance due to Compton effect from higher energy gamma-rays), to fall into 13 specified energy positions, within 1 keV is: $\binom{14}{13} p^{13}(1-p)^{(14-13)} = 4.1 \times 10^{-8}$, where p is equal to $(36 \times 1.0)/(250 - 90)$. The number of possible gamma-transitions between states of both integer and half integer spins with $E_x = 4.42 \times J(J+1)$, in the range of 90 to 250 keV is 36.

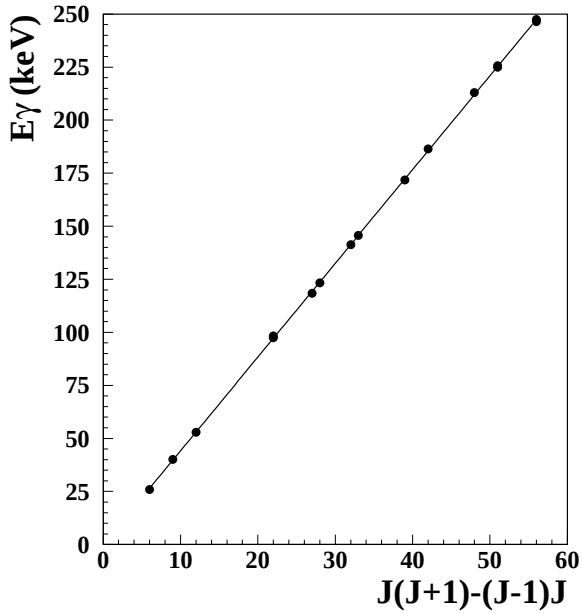

Fig. 11. E_γ versus $J(J+1) - (J-1)J$ for the γ-rays seen in coincidence with 7.8–8.6 MeV α-particles in measurements I and II. (Circled events in Figs. 5 and 6, see Table 2(a).)

Table 2. The energies of the γ-rays in coincidence with (a) 7.8–8.6 MeV and (b) 6.0–7.0 MeV α-particles (the circled events in Figs. 5 and 6), as compared to calculated transitions assuming $E_x = E_0 \times J(J+1)$.

E_α (MeV)	E_γ(expt.)[a] (keV)	E_γ(cal.) (keV)	ΔE (keV)	Transition[b]
a) $E_\alpha = 7.8$–8.6 MeV; $E_x = 4.42 \times J(J+1)$ keV				
7.81	25.9	26.5	−0.6	$3 \to 2$
8.52	40.1	39.8	+0.3	$9/2 \to 7/2$
8.21	52.9	53.0	−0.1	$6 \to 5$
8.53[c]	97.9[c]	97.2	+0.7	$11 \to 10$
8.19	118.4	119.3	−0.9	$27/2 \to 25/2$
7.88	123.4	123.8	−0.4	$14 \to 13$
8.37	141.3	141.4	−0.1	$16 \to 15$
7.99	145.6	145.9	−0.3	$33/2 \to 31/2$
8.51	171.8	172.4	−0.6	$39/2 \to 37/2$
8.60	186.5	185.6	+0.9	$21 \to 20$
8.07	212.9	212.2	+0.7	$24 \to 23$
8.59[d]	225.3[d]	225.4	−0.1	$51/2 \to 49/2$
8.61[e]	247.0[e]	247.5	−0.5	$28 \to 27$
b) $E_\alpha = 6.0$–7.0 MeV; $E_x = 4.41 \times J(J+1)$ keV				
6.16	176.1	176.4	−0.3	$20 \to 19$
6.94	207.4	207.3	+0.1	$47/2 \to 45/2$
6.41	242.3	242.6	−0.3	$55/2 \to 53/2$

[a]The peak to total ratio was 100% up to about 120 keV and reduced gradually to 22% at 250 keV.
[b]The transitions between the maximum possible spins are given. At relatively high energies the observed γ-rays are most probably sum events due to various combinations of lower energy transitions in the band which, because of the $J(J+1)$ law, fit in energy to calculated transitions between higher energies. (see text).
[c]Average of two events: 8.47 MeV α in coincidence with 97.4 keV γ in the first measurement and 8.58 MeV α in coincidence with 98.3 keV γ in the second measurement.
[d] Average of two events: 8.61 MeV α in coincidence with 224.9 keV γ in the first measurement and 8.57 MeV α in coincidence with 225.7 keV γ in the second measurement.
[e]Average of two events in the second measurement of 8.62 MeV α in coincidence with 246.5 keV γ and 8.60 MeV α in coincidence with 247.5 keV γ.

(The four low energy events of $E_\gamma \leq 60$ keV in Fig. 5 and the one event in Fig. 6 which do not fit with the $J(J+1)$ rule may be due to Compton events.) It is also seen in Fig. 6 and in Table 2(b) that the γ-rays of the 3 coincidence events in the region of 6–7 MeV α-energy, of $E_\alpha = 6.16$ MeV–$E_\gamma = 176.1$ keV, $E_\alpha = 6.94$ MeV–$E_\gamma = 207.4$ keV and $E_\alpha = 6.41$ MeV–$E_\gamma = 242.3$ keV, fit with $20 \to 19$ (176.4), $47/2 \to 45/2$ (207.3) and $55/2 \to 53/2$ (242.6) $J \to J-1$ transitions, assuming $E_x = 4.41 \times J(J+1)$ keV. The probability in this case that this fit is accidental

due to a chance coincidence of evenly distributed events is 1.2×10^{-3}, taking into account that $p = (18 \times 0.47)/(250 - 170)$, 18 is the number of possible gamma-transitions in the range of 170 to 250 keV, and 0.47 keV is twice the average deviation from the specified energies. (This probability increases to 1.1×10^{-2} if, instead of 0.47 keV, the value which was used before of 1.0 keV is assumed in the calculation.) It should be mentioned that rotational constants around 4.4 keV correspond to superdeformed bands (SDB) in this region of nuclei.[8]

In Fig. 9 one sees about 10 scattered events in the 6.5–9 MeV region. Some of them may also fit with a $J(J+1)$ law. However, the statistical significance of the fit in this case is not so high and we will not discuss them further.

The appearance in Table 2(a) of both integer and half-integer spins at low γ-ray energies indicates that bands in both even and odd nuclei were formed.[d] (At high energies the observed transitions are probably sum events. See the following paragraphs.) ^{207}Rn, produced via pn evaporation, and its daughters, are, from the kinematic point of view, the best candidates for the half-integer transitions. The 8.42 MeV α-particle in coincidence with a photon of 67.1 keV (seen in Fig. 5 and Table 3), which fits with $K_{\alpha 1}$ X-ray of Pt (known energy 66.832 keV), may indicate that the α-transition is from ^{195}Hg to ^{191}Pt. ^{195}Hg is the daughter after three α-particle decays from ^{207}Rn.[e]

It should be mentioned that the high energy γ-rays (above about 120 keV, Table 2) are most probably sum events rather than photo-peak events. If, for instance, the three coincidence events in Fig. 6 at E_γ of 247.0 (two events) and 225.3 keV are photo-peak events, then 9.5±5.5 Compton events below 120 keV (the position of the Compton edge) should have been seen in coincidence with α-particles of 8.55–8.61 MeV, but only one event is seen. Similarly if the γ-rays which are in coincidence with 6–7 MeV α-particles, seen in the same figure and mentioned above, are photo-peak events, then 7.6 ± 4.4 Compton events should have been seen in this α-energy range at $E_\gamma \leq 120$ keV, while only one event is seen. On the other hand, for a de-excitation of a superdeformed band with $\Delta J = 1$, a measured energy which fits a transition between high-spins, may be due to many sum combinations of lower energy transitions between lower spins, for which low-energy Compton events should not be observed. For instance, an energy of 225.4 keV which fits a $51/2 \rightarrow 49/2$ transition (assuming $E_x = 4.42 \times J(J+1)$ keV, Table 2) may be due to one of 17 different combinations of 3-fold events, if only the first 14 levels of the band up to maximum spin of 27/2 and maximum transition energy of 119.3 keV are considered, for which the photo-peak to total ratio is 100%. (119.3 $(27/2 \rightarrow 25/2)$ + 92.8 $(21/2 \rightarrow 19/2)$ + 13.3 $(3/2 \rightarrow 1/2)$ = 225.4, or 84.0 $(19/2 \rightarrow 17/2)$ + 75.1 $(17/2 \rightarrow 15/2)$ + 66.3 $(15/2 \rightarrow 13/2)$ = 225.4 are two examples out of these 17 possible combinations.) Because of the large

[d]It should be mentioned that identical bands in neighboring nuclei are known.[18]
[e]The α-transitions from ^{207}Rn to ^{195}Hg are not normal transitions but presumably hyperdeformed to hyperdeformed transitions (see Sec. 4.4).

solid angle of the γ-detector (0.16) and the large number of possible 3-fold combinations, the probability P_3 to see a 3-fold event is larger than the probability P_1 to see a 1-fold event. (These probabilities for the above example are: $P_1 = \epsilon'(1-\epsilon)^{(N-1)} = 0.042(1-0.16)^{24} = 6.4 \times 10^{-4}$, and $P_3 = n_3\epsilon^3(1-\epsilon)^{N-3} = 17 \times 0.16^3(1-0.16)^{10} = 1.2 \times 10^{-2}$, about 20 times larger. ϵ' is the photo-peak efficiency of the detector for the particular energy, ϵ is the geometrical efficiency, N is the number of transitions in the band counting from the level to which the α-particle is decaying, and n_3 is the number of 3-fold combinations).

Many combinations of 2- or 4-fold events of a half-integer spin band will give energies which fit with those of a band of an integer spin. For instance, the two events at 247.0 keV (Table 2) which fit in energy to a $28 \rightarrow 27$ transition, and the 186.5 keV event which fits with a $21 \rightarrow 20$ transition, may be due to such combinations, since the α-particle energy is the same as that of the half-integer transitions of 225.3 and 171.8 keV, and therefore they presumably belong to the same band. (In an integer-spin band of $\Delta J = 1$ various combinations of 2-, 3- and 4-fold events of low energy transitions have large efficiencies and give energies which fit with those of transitions between higher spins. This property, both for half-integer and integer spin bands, does not exist for $\Delta J = 2$ transitions.)[f,g]

As shown above, the detection of sum events which are energetically degenerate with the diagram line leads to a substantially increased effective detection efficiency (dependent, however, on the maximum available spin) for this energy. By binning the data of Table 2(a), where the intensity of the γ-rays which fit with energies to transitions between relatively high spins (from $16 \rightarrow 15$ up to $28 \rightarrow 27$ transitions) is larger than between low spins, and taking into account the effective detector efficiency for various 1-, 2-, 3-, 4- and 5-fold sum events, one sees that the data fit best if the α-particle decays to a 39/2 state. The estimated lower limit of the maximum produced spin is 25/2, while, because of the low statistics, the higher limit is not well defined.

The deduced production cross section depends on the effective efficiency of the detector and hence on the assumed maximum produced spin. It is about 12 nb (shown in Table 1) for a maximum spin of 39/2 and about a factor of two lower for a maximum produced spin of 25/2. As shown above, the observation in Table 2 of gamma rays which fit in energies with transitions between high spin SDB states is consistent with various sums of gamma rays due to transitions between lower spin states with $\Delta J = 1$. Since the intensity of the characteristic X-rays (or various sums

[f]Previously,[15,16] it was assumed that the 247.0 (2 events), 225.3 (2 events) and 191.7 keV events, which are in coincidence with 8–9 MeV α-particles, are photo-peak events due to known transitions in ^{195}Hg and ^{197}Tl. However, in this case 12.6 ± 6.3 Compton events below 120 keV should have been seen in Fig. 6 in coincidence with α-particles of 8.55–8.62 MeV, but only one event is seen.

[g]In principle one may think that the observed high-energy γ-rays are Compton events due to even higher energy γ-rays. But then the probability[8] to have two events in the same position (within the energy resolution) is only a few percent, and this occurred twice, at 247.0 (Fig. 6) and 225.3 keV (Figs. 5 and 6).

of them) seen in Figs. 5 and 6 in coincidence with 8–9 α-particles is very low (one event), the observed γ-rays should be due to E1 transitions, with quite low internal conversion factors, rather than M1 ones.[h] Such transitions have been seen before[8] and were predicted for SD wells in nuclei around $Z = 86$ and $N = 116$.[20–22]

3.3. *Coincidences between α-particles and characteristic X-rays and identified γ-rays*

In order to identify some of the coincidence events seen in Figs. 5, 6, and 9 at lower particle energies below 6 MeV, we first looked at groups of events. The existence of groups of three or two coincidence events in clean regions indicates that they are probably not background. Secondly, one looks at their accurately measured photon energies. At low energies the observed photon may be either an X-ray or a γ-ray. The energies of the characteristic X-rays of the elements are known very well.[25] The $K_{\alpha 1}$ X-rays of the various elements of the evaporation residue nuclei and their daughters are separated from one another by about 2 keV, where the value of a $K_{\alpha 1}$-line of an element with Z protons is about the same as the value of the $K_{\alpha 2}$-line of an element with $Z + 1$ protons. If the measured energy turns out to be very close to a known X-ray energy, then it is reasonable to assume that the observed photon is an X-ray rather then a γ-ray. (In the cases found by us and discussed below the deviations from the known values are from 0.03 to 0.28 keV, while the width of one channel in the γ-spectrum is about 0.24 keV and the FWHM is about four channels.) The X-ray may be emitted if the α-particle is decaying to an excited state which decays by conversion electrons. Such a process is followed by emitting characteristic X-rays of the daughter nucleus. The Z-value of the daughter is thus determined. In order to determine its A-value we tried to identify the γ-rays which are in coincidence with α-particles of about the same energy. A consistency is obtained when the γ-ray fit in energy with the measured value, belongs to an isotope of the determined element, and it is consistent with known or expected values of the conversion factors, and also with the decay scheme.

In several cases, as seen below, some of the observed events have been identified as due to characteristic X-rays (the events surrounded with squares in Figs. 5, 6 and 9) and as known γ-transitions in various nuclei (the events surrounded with triangles in Figs. 5, 6 and 9). In Fig. 6 two coincidences between about 5.50 MeV α-particles and 61.1 and 59.4 keV photons are seen, and fit with $K_{\alpha 1}$ and $K_{\alpha 2}$ X-rays of Re of 61.140 and 59.718 keV. At about the same α-energy two 144.0 keV events are observed and can be identified with a known transition in ^{186}Re. This identification is supported by the observation in Fig. 5, in the same α-energy range, of coincidence events with respective 59.7 keV and 140 keV X- and γ-rays. The first

[h]The internal conversion coefficient in the K-shell for E1 γ-ray transition of about 130 keV in Pt is about 0.2, and for M1 transition is about 3.[19] If the γ-rays are of M1 character then 11 or 4 transitions respectively, should have been strongly converted for maximum spin of the band of 39/2 or 25/2.

fits with $K_{\alpha 2}$ of Re, and the second with a transition in ^{186}Re, which precedes the above 144.0 keV transition. A coincidence between 5.45 MeV α-particles and 59.4 or 59.7 keV photons may in principle be also due to the known decay of ^{241}Am of 5.486 MeV α and 59.54 keV γ. However, we did not use and never had in our laboratory a ^{241}Am calibration source. Under these circumstances the observation of the 61.1 keV photon, which fits very nicely with $K_{\alpha 1}$ of Re, and which is very far off (1.56 keV) from the γ-rays of ^{241}Am, and of the two consecutive γ-rays of ^{186}Re, suggests that the two events at about 59.6 keV are due to $K_{\alpha 2}$ of Re and not due to ^{241}Am. A 59.6 keV X-ray may in principle be also due to $K_{\alpha 1}$ of W of 59.3182 keV. Here also the observation of the other X-rays and γ-rays suggest that it is $K_{\alpha 2}$ of Re rather than $K_{\alpha 1}$ of W. Out of total number of 3 X-rays, one is expecting to see 1.9 $K_{\alpha 1}$ events and 1.1 $K_{\alpha 2}$ events. The observation of one event in the first case and two in the second, is well within the statistical error.

In Fig. 9, for α-particles between 5.18 and 5.53 MeV, groups of two and three events with photon energies of 66.8 keV and 59.6 keV, respectively, are seen. They may correspond to the known $K_{\alpha 1}$ X-rays of Pt of 66.832 keV and of W of 59.318 keV. At the same corresponding α-energies known γ-rays of ^{189}Pt and ^{183}W are observed. Here the three 59.6 keV events are more likely to be due to $K_{\alpha 1}$ of W, rather than $K_{\alpha 2}$ of Re. If they were $K_{\alpha 2}$ of Re then 5.2 events of $K_{\alpha 1}$ at 61.140 keV are expected. The observation of zero events when five are expected is unlikely. On the other hand, if the three observed events are $K_{\alpha 1}$ X-rays of W, then 1.7 events of $K_{\alpha 2}$ of W at 57.98 keV are expected. The observation of zero events when 1.7 are expected is well within statistical errors.

As mentioned above and seen in Table 3, about the same α-energy corresponds to two different decays. One leads to ^{186}Re and was obtained in the $E_{\mathrm{Lab}} = 125$ MeV experiment, and the other presumably leads to ^{183}W and was obtained in the $E_{\mathrm{Lab}} = 135$ MeV experiment. As seen below (Sec. 4.1), these data are interpreted as due to transitions from the second well of the potential in the parent nuclei to the normal states in the daughters. There is nothing against having about the same α-particle energy in two different transitions. Because of the low statistics we consider the identifications mentioned above as tentative only, where the identification of ^{186}Re, which is based on six coincidence events, is better than that of the other isotopes.

The results are summarized in Table 3 together with possible reaction channels and corresponding decay chains which lead to the observed transitions. The deduced production cross sections (with an accuracy of about a factor of two) are given in Table 1, columns 3 and 5. In general, lower limits were deduced since the branching ratios along the decay chains are not known.

Some coincidence events between 6.17–9.01 MeV α-particles and identified X-rays with no corresponding γ-rays were seen. They are also given in Table 3.

Table 3. Summary of tentatively identified X- and γ-rays which were in coincidence with various particles in measurements I and II (125 MeV) and measurement III (135 MeV). In column 1 we give the measured γ-energies, their times of occurrence from the beginning of the measurement or estimated half-life if several events are observed (bold letters), and the measurement number. In column 2 the respective particle energies are given. Column 3 are the tentatively identified nuclei with the character of transition in column 4.[25] The fifth column gives the possible reaction channel and the decay chain (bold letters) to the identified mother isotope. (More complicated situations are in principle not impossible. See text, Sec. 4.2.) The sixth column shows lower limits on the excitation energies of the decaying isomeric states in the mother nuclei (in brackets). Theoretical predictions for the excitation energies of the second minima (s.m.) in the mother nuclei given by Satula *et al.* (S, Ref. 10) and Krieger *et al.* (K, Ref. 11) are in the last column. (For the last case a prediction[27] for the third minimum is given).

E_γ(Meas. No.)	$E_{\alpha,p}$	Isotope	Transition	Reaction	$E_x^{\text{i.s.}}(^{\text{A}}\text{Z})$	$E_x^{\text{s.m.}}$
keV	MeV			**Decay**	MeV	MeV
Time/d[a]				**Chain**		S; K
61.1(II)	5.48		$K_{\alpha 1}$(Re)			
31.1						
59.6(x2)(I; II)	5.45		$K_{\alpha 2}$(Re)			
7.4; 107.2						
144.0(x2)(II)	5.43	^{186}Re	330(?)[b] $\rightarrow$ 186	3n	$\geq 3.1(^{190}\text{Ir})$	4.1[d]; 4.2[d]
60.2; 88.8			$(5^+) \rightarrow (6)^-$	**4α,**		
			E1; 100%	**2β^+(EC)**[c]		
141.0(I)	5.29	^{186}Re	471(?)[b] $\rightarrow$ 330(?)[b]	3n	$\geq 3.2(^{190}\text{Ir})$	4.1[d]; 4.2[d]
130.2			$(4^+) \rightarrow (5^+)$	**4α,**		
			M1 + E2	**2β^+(EC)**[c]		
66.8(x2)(III)	5.18		$K_{\alpha 1}$(Pt)			
13.9; 58.6						
236.2(III)	5.12	^{189}Pt	2291.8 $\rightarrow$ 2056.1	p3n; 4n	≥ 4.53 (^{193}Hg)	4.2[e]; 4.6[e]
139.5			$(\frac{29}{2}^+) \rightarrow (\frac{27}{2}^-)$	**3α; 3α,**		
			(E1)	— ; **β^+(EC)**[c]		
59.6(x3)(III)	5.53		$K_{\alpha 1}$(W)			
$\mathbf{t_{1/2} = 90}$						
210.3(III)	5.43	^{183}W	308.9 $\rightarrow$ 99.1	α2n	$\geq 3.04(^{187}\text{Os})$	3.4[d]; 3.6[d]
168.4			$\frac{9}{2}^- \rightarrow \frac{5}{2}^-$	**4α,**		
			E2; 100%	**β^+(EC)**[c]		
70.9(II)	9.01		Kα_1(Hg)			
89.7						
67.1(I)	8.42		Kα_1(Pt)			
81.7						
79.1(I)	6.17		Kα_1(Po)			
133.5						
13.9(II)	7.16		Lβ_1(At)			
64.6						

Table 3. (*Continued*)

13.9(III)	7.05		$L\beta_1$(At)			
127.8						
185.8(x3)(III)	3.88(p)	^{204}Rn	2219.0 → 2032.8[f]	4n	≥ 6.7(^{205}Fr)	3.9[e]; 5.0[e]
$\mathbf{t_{1/2} = 120}$			$(9^-) \rightarrow (8^+)$	–		
			E1; 55%			
SDB(II)[g]	6 - 7	^{203}Po	SDB	pn	7.8[h];10.3[i](^{207}Rn)	6.8[d]; 9.9[e]
$\mathbf{t_{1/2} = 53}$			Table 2(b)	–		
SDB(I; II)[j]	8.6	^{191}Pt[k]	SDB	pn	∼12.5(^{195}Hg)[k]	11.5($^{\text{III min}}$)[l]
$\mathbf{40 \leq t_{1/2} \leq 765}$			Table 2(a)	$\boldsymbol{3\alpha}$		

[a]For a group of three events, the half-lives as estimated according to the formulas of K.-H. Schmidt *et al.*[23] are given.
[b]The excitation energy in ^{186}Re is not certain.[25]
[c]The order of the decay is not known.
[d]Extrapolated value.
[e] Interpolated value.
[f]The identification given in the table is not certain, as explained in the text.
[g]See text and Table 2(b) for the γ-energies of this band.
[h]Estimated excitation energy in ^{207}Rn assuming E_α = 6.5 MeV, a predicted E_x of the second minimum in ^{203}Po of 6.6 MeV,[10] and decay to a SDB state with a spin of 27/2 at excitation energy above the second minimum of 863 keV.
[i]As comment (h) above except that E_x of the second minimum in ^{203}Po was taken at 9.1 MeV as predicted in Ref. 11.
[j]See Table 2(a) for the γ-energies of this band.
[k]See Sec. 4.4.
[l]Extrapolated value for the excitation energy of the third minimum from Ref. 27 is given.

3.4. *Evidence for proton radioactivity*

A very well-defined coincidence group of three events is seen in Fig. 9 at an average particle energy of 3.88 MeV and γ-energy of 185.8 keV. Because of the low energy of the particles and the very narrow total width of 40 keV, one may conclude that the particles are protons. (The total estimated widths at this energy are 55 keV for protons and 630 keV for α-particles. The estimated half-life for 3.88 MeV α-particles decaying to, for instance, ^{194}Hg is about 1×10^8 y [7]). The 185.8 keV γ-rays fit with a known transition in ^{204}Rn (Table 3). The production cross section of this group is given in Table 1.

4. Discussion

4.1. *Transitions from superdeformed to normal states*

The E_α values for the g.s. to g.s. transitions for ^{190}Ir → ^{186}Re; ^{187}Os → ^{183}W and ^{193}Hg → ^{189}Pt mentioned in Table 3 are 2.74, 2.662 and 2.927 MeV,[24] respectively. The corresponding observed α-energies of 5.43, 5.53 and 5.18 MeV (Table 3) are

clearly due to the decay of isomeric states in the parent nuclei. The estimated half-lives for normal α-particles of these energies[7] are 2.9×10^3; 3.5×10^2 and 1.2×10^6 s. The observed lifetimes of several months, which may be due to combined lifetimes along the long decay chains, are retarded by three and four orders of magnitude in the first and second case, respectively.

From the above mentioned measured α-energies the lower limits for the excitation energies of the isomeric states in the parent nuclei ^{190}Ir, ^{187}Os and ^{193}Hg (see Table 3) are deduced to be 3.1; 3.0 and 4.5 MeV, respectively. (Lower limits are deduced since the α-decay may proceed through a higher excitation energy than that seen experimentally.) Extrapolated and interpolated predicted energies[10,11] for the second minima of 4.1[10] or 4.2[11]; 3.4[10] or 3.6[11]; and 4.2[10] or 4.6[11] MeV, respectively, are also given in Table 3. The observed energies of the isomeric states and the predicted positions of the second minima seem to be in the same range of excitation energies. This suggests that the isomeric states in these cases are in the second well of the potential, and that the α transitions are from the superdeformed well in the parent nuclei to less deformed or normal states in the daughters. These are the last transitions after several decays, presumably from isomeric state to isomeric state, all within the second wells along the decay chain. For instance, ^{190}Ir in the isomeric state may be produced after six decays, 4α and $2\beta^+$ or EC decays, all from superdeformed to superdeformed states (see Table 3).[i] Since the last step of the chain is a decay to a relatively high spin state, it seems that the originally produced isomeric state in the evaporation residue nucleus has high spin, and that the transitions from mothers to daughters along the decay chain are between high spin states.

4.2. *Transitions from superdeformed to superdeformed states?*

We now discuss the three coincidence events seen in Fig. 6 and mentioned above (Sec. 3.2 and Table 2(b)) of 6.16 MeV (α)–176.1 keV (γ); 6.94 MeV (α)–207.4 keV (γ) and 6.41 MeV (α)–242.3 keV (γ). These events appeared 96, 68 and 78 days respectively, after the end of irradiation, and their lifetimes therefore are of the order of several months. As shown above, the energies of the last two γ-rays fit very nicely with SDB transitions between half-integer spins, where the most probable candidates are ^{207}Rn, produced by the pn evaporation process, and its daughters. The coincidence event of a 6.17 MeV α-particle with 79.1 keV photon (Fig. 5 and Table 3) which fits with Po $K_{\alpha 1}$ X-rays of 79.290 keV, suggests that the transitions mentioned above with 6–7 MeV α-particles might be from isomeric state(s) in ^{207}Rn to the SDB states in the second well of the potential in ^{203}Po. (The half-life of the ground state of ^{207}Rn is 9.3 mn.) The measured α-particle energies are in the

[i]More complicated situations where the evaporation residue nucleus is produced in the third (hyperdeformed) well of the potential, and then decays to the second well by α-particle or even by proton emission, is in principle not impossible.

predicted range for the transition from the second minimum in ^{207}Rn to the second minimum in ^{203}Po of 6.2[10] or 6.9[11] MeV.

Similarly the energies of 7.16 MeV (Fig. 6; $E_{\rm Lab}$ = 125 MeV) and 7.05 MeV (Fig. 9; $E_{\rm Lab}$ = 135 MeV) α-particles in coincidence with $L_{\beta 1}$(At) (see Table 3) may correspond to the predicted α-particle transitions between the second minima of ^{206}Fr$^{\rm s.m.}$ and ^{202}At$^{\rm s.m.}$ (3n reaction) of 6.9[10] or 7.3[11] MeV, and of ^{205}Fr$^{\rm s.m.}$ to ^{201}At$^{\rm s.m.}$ (4n reaction) of 7.0[10] and 7.2[11] MeV, respectively.

In both cases discussed in the present subsection, while the α-energies are consistent with this picture, the very long lifetime may indicate that the internal structure of the parent isomeric states and the final rotational SDB states are different.

4.3. *Proton transition from a superdeformed to a normal state?*

For the 3.88 MeV proton group (Sec. 3.4 above), if the identification given in Table 3 is correct, the excitation energy of the isomeric state in ^{205}Fr is $\geq$ 6.7 MeV (see Table 3). This is quite high compared to 3.9[10] or 5.0[11] MeV predicted for the second minimum, and may indicate that the origin of the isomeric state in this case is different.

4.4. *Hyperdeformed to superdeformed transitions*

The most striking result is the α-particle group around 8.6 MeV which was found in coincidence with SDB transitions (Figs. 5–8, and Table 2(a)). As mentioned above the appearance of γ-transitions between half-integer spins shows that most of these transitions are in an odd A nucleus, where ^{207}Rn and its daughters are most probable candidates from the reaction kinematic point of view.[j] The observation of a coincidence event between a 8.42 MeV α-particle (which is, within the experimental spread for α-particles, consistent with 8.6 MeV for 200 μg/cm^2 C catcher foil) and a $K_{\alpha 1}$ X-ray of Pt (Fig. 5 and Table 3) indicates that the transition may be from ^{195}Hg (produced after three α-decays from ^{207}Rn) to ^{191}Pt.[k] However, transitions from other Hg isotopes produced by fewer α-decays, which are followed by several β^+ or EC decays cannot be excluded.

The predicted[7] half-life for normal 8.6 MeV α-particles is below 1 μs. Therefore in principle the γ-rays of the SDB transitions may either precede or follow the 8.6 MeV α-particles.[l] In the case where the γ-rays come first, the α-particles are due to either a transition from the second minimum in the parent nucleus to the second minimum in the daughter, or from the second minimum in the parent to

[j] As shown in Sec. 3.2. above, the high energy integer spin transitions of 247.0 and 186.5 keV (Table 2(a)) are presumably due to sum combinations of half-integer transitions as well.

[k] As mentioned in footnote "e" and discussed below, the three α-transitions from ^{207}Rn to ^{195}Hg are presumably hyperdeformed to hyperdeformed transitions.

[l] In all the cases discussed above the first possibility is excluded since the lifetime of the α-particles is always much longer than 1 μs, and they could not be detected in coincidence with γ-rays which precede them.

normal states in the daughter. However, in the first case the energy of 8.6 MeV is much larger than the predicted 3.3 MeV in $^{195}Hg^{s.m.} \rightarrow {}^{191}Pt^{s.m.}$ transition,[10,11] and 6.3[10] or 6.9[11] in $^{207}Rn^{s.m.} \rightarrow {}^{203}Po^{s.m.}$ transition. On the other hand in the second case of an α-transition from the second minimum to normal states, the α-particle lifetime will most probably be retarded, and the 8.6 MeV α-particles will not be in coincidence within 1 μs with the SDB transitions. (Furthermore, the predicted transition energy from the second minimum to the ground state in $^{195}Hg^{s.m.} \rightarrow {}^{191}Pt^{g.s.}$ is about 7.2 MeV[10,11] and in $^{207}Rn^{s.m.} \rightarrow {}^{203}Po^{g.s.}$ is 6.3[10] or 6.9 MeV.[11] These values are also not in accord with the experimental value of 8.6 MeV).

It is therefore reasonable to assume that the 8.6 MeV α-particles decay first and then are followed by the SDB γ-rays, similar to the situation in all the other cases discussed above. Let us first consider the case where the isomeric state is in the second well of the parent nucleus which decays by the 8.6 MeV α-particles to the SDB in the daughter. One faces two problems here, namely the very large hindrance factor of the α-particles, and their high energy. The hindrance factor of the α-particles is in the range of 10^{16} ($t_{1/2} \sim 40$ d as compared to the predicted value of 1.4×10^{-10} s assuming $\beta_2 = 0.7$[8]). As for the energy, if, for instance, the 8.6 MeV α-particles decay to a SDB state of spin 39/2 in ^{191}Pt at $E_x = 1.77$ MeV ($E_0 = 4.42$ keV), and taking into account the predicted excitation energy of the second minimum in ^{191}Pt at about 4.1 MeV,[10,11] and the Q_α(g.s. $\rightarrow$ g.s.) value for ^{195}Hg of 2.190 MeV,[24] the isomeric state in ^{195}Hg turns out to be at about 12.5 MeV above the g.s. Assuming an excitation energy of the second minimum in ^{195}Hg of about 5.2 MeV,[10,11] the above energy of 12.5 MeV corresponds to an excitation energy of about 7.3 MeV above the second minimum, which seems unlikely. (In the same way, about 6.0 and 4.0 MeV excitation energies above the second minimum are respectively deduced for more neutron-rich Hg isotopes and for ^{207}Rn, which is unlikely as well.)

It seems reasonable to conclude that the large hindrance factor might be due to another barrier transition, as, for instance, from the third well (the hyperdeformed well)[26–28] to the second one.[m] It should be mentioned that an extrapolated value of about 11.5 MeV is obtained for the excitation energy of the third minimum in ^{195}Hg from the predictions of Ref. 27. This value is in accord with the deduced value mentioned above of about 12.5 MeV.[n]

The predicted[27] excitation energy of the third minimum in this region of nuclei is several MeV above the second minimum. The originally produced isomeric state in ^{207}Rn should therefore be an isomer in the third minimum which then decays

[m]It should also be mentioned that a superdeformed minimum on the oblate side, which might decay to the prolate superdeformed minimum via triaxial shapes, has been predicted in ^{236}Cm at $\beta_2 = -0.63$ and $E_x = 8.2$ MeV, using Hartree–Fock calculations.[29]

[n]The retardation of the α-events of 6–7 MeV discussed in Sec. 4.2 is unlikely to be due to transitions from the third minimum, as its predicted excitation energy of about 18.8 MeV (extrapolated from Ref. 28) comes out far from the data of 7.8 or 10.3 MeV (Table 3).

by three consecutive α-particle third minimum to third minimum transitions to the isomeric state in ^{195}Hg. (Transitions from the second or first minima to the third minimum are very unlikely since in these cases the α-energy will be several MeV below the g.s. to g.s. transition.) Since the hyperdeformed isomeric state in ^{195}Hg decays to a superdeformed high spin in ^{191}Pt, all the transitions from ^{207}Rn down to ^{195}Hg should be between high spin states as well.

It is seen in Table 1 that while the highest cross section for the production of the normal evaporation residue nuclei is about a factor of 60 larger at 135 MeV as compared to 125 MeV, the production of the isomeric states in the second minimum is about the same at these two bombarding energies, while the isomeric state in the third minimum, which was produced with somewhat larger cross section, was observed only at the lower bombarding energy of 125 MeV.

5. Summary

In summary, evidence for long-lived isomeric states with lifetimes of up to several months, with abnormal decay properties, was obtained. Relatively high energy α-particles of 5.1–5.5 MeV were tentatively found in the usually non-α-emitting nuclei, ^{187}Os, ^{190}Ir and ^{193}Hg, and interpreted as due to transitions from the second well of the potential in the parent nuclei to less deformed or normal states in the daughters. The observed transitions are the last in long chains of up to six steps of α-particle and β^+ or EC transitions, presumably within the second well itself.

Long-lived 6–7 MeV α-particles, in coincidence with SDB γ-rays, were found with energies consistent with transitions from the second minimum in the parent nucleus to the second minimum in the daughter. The reason for their long lifetimes though is not clear.

A 3.88 MeV long-lived proton group was found. Its state of origin is not entirely clear.

By far the most exciting observation is the very high energy and strongly retarded (40 d $\leq t_{1/2} \leq$ 2.1 y) 8.6 MeV α-particle group in coincidence with SDB transitions, which is interpreted as due to a long-lived isomeric state in ^{195}Hg at $E_x \cong 12.5$ MeV, and is consistent with a transition from the third (hyperdeformed) well of the parent nucleus to the second (superdeformed) well in the daughter.

The production cross sections of the isomeric states in the second well were about the same at $E_{\mathrm{Lab}} = 125$ (10% below the barrier) and at $E_{\mathrm{Lab}} = 135$ MeV. Somewhat larger cross section was found for the production of the high-spin isomeric state in the third minimum which was found only at the lower bombarding energy of 125 MeV.

The existence of such long-lived isomeric states, with lifetimes much longer than those of their corresponding ground states, and with preferential production cross sections at relatively low bombarding energies even below the Coulomb barrier, may add new considerations regarding the stability and the production mechanism of heavy and superheavy elements.[3,30–32] In particular it should be mentioned that in

terms of the extra-push model, the extra-push energies needed for the production of such nuclei in their superdeformed and hyperdeformed wells are much smaller than expected for producing them in their normal states.[33]

Acknowledgements

We acknowledge the support of the accelerator crew of the Weizmann Institute at Rehovot, and the technical assistance of S. Gorni, O. Skala and the electronic team of the Racah Institute. D. K. acknowledges the financial support of the DFG. We are grateful to N. Zeldes and J. L. Weil for very valuable discussions.

References

1. A. Marinov, S. Eshhar and D. Kolb, *Phys. Lett.* **B191** (1987) 36.
2. A. Marinov, S. Eshhar and J. L. Weil, *Proc. Int. Symp. on Superheavy Elements*, Lubbock, Texas, 1978, ed. M. H. K. Lodhi (Pergamon, New York, 1978) p. 72.
3. A. Marinov, C. J. Batty, A. I. Kilvington, G. W. A. Newton, V. J. Robinson, and J. D. Hemingway, *Nature* **229** (1971) 464.
4. A. Marinov, S. Eshhar and D. Kolb, *Fizika* **19**, Supplement 1 (1987) 67.
5. A. Marinov, *6th Adriatic Int. Conf. on Nucl. Phys.*, *Frontiers of Heavy-Ion Physics*, 1987, eds. N. Cindro, W. Greiner and R. Ćaplan (World Scientific, 1987) p. 179.
6. A. Marinov, S. Gelberg and D. Kolb, *Int. Symp. on Exotic Nuclear States*, Debrecen, Hungary, 1997, eds. Zs. Dombrádi, Z. Gásci and A. Krasznahorkay, APH N.S., *Heavy Ion Physics* **7** (1998) 47.
7. V. E. Viola Jr. and G. T. Seaborg, *J. Inorg. Nucl. Chem.* **28** (1966) 741.
8. A. Marinov, S. Gelberg and D. Kolb, *Mod. Phys. Lett.* **A11** (1996) 861.
9. A. Marinov, S. Gelberg and D. Kolb, *Mod. Phys. Lett.* **A11** (1996) 949.
10. W. Satula, S. Ćwiok, W. Nazarewicz, R. Wyss, and A. Johnson, *Nucl. Phys.* **A529** (1991) 289.
11. S. J. Krieger, P. Bonche, M. S. Weiss, J. Meyer, H. Flocard, and P.-H. Heenen, *Nucl. Phys.* **A542** (1992) 43.
12. S. G. Nilsson, G. Ohlén, C. Gustafson, and P. Möller, *Phys. Lett.* **30B** (1969) 437.
13. J. Fernández-Neillo, C. H. Dasso and S. Landowne, Code CCDEF, *Comp. Phys. Comm.* **54** (1985) 409.
14. S. Raman, C. H. Malarkey, W. T. Milner, C. W. Nestor Jr., and P. H. Stelson, *At. Data and Nucl. Data Tables* **36** (1987) 1.
15. A. Marinov, S. Gelberg and D. Kolb, *Proc. Int. Workshop on Physics of Unstable Nuclear Beams*, São Paulo, Brazil, 1996, eds. C. A. Bertulani, L. F. Canto and M. S. Hussein (World Scientific, 1996) p. 181.
16. A. Marinov, S. Gelberg and D. Kolb, *Int. School-Seminar on Heavy Ion Physics*, Dubna, Russia, 1997, eds. Yu. Ts. Oganessian and R. Kalpakchieva (World Scientific, 1998) p. 437.
17. A. Marinov, S. Gelberg, D. Kolb, and J. L. Weil, *Proc. 2nd Int. Conf. on Fission and Properties of Neutron Rich-Nuclei*, St. Andrews, Scotland, 1999, eds. J. H. Hamilton, W. R. Phillips and H. K. Carter (Word Scientific, 2000) p. 231.
18. F. S. Stephens *et al.*, *Phys. Rev. Lett.* **65** (1990) 301.
19. F. Rösel, H. M. Fries, K. Alder, and H. C. Pauli, *At. Data and Nucl. Data Tables* **21** (1978) 291.
20. S. Åberg, *Nucl. Phys.* **A520** (1990) 35c.

21. J. Höller and S. Åberg, *Z. Phys.* **A336** (1990) 363.
22. W. Nazarewicz, P. Olanders, I. Ragnarsson, J. Dudek, and G. A. Leander, *Phys. Rev. Lett.* **52** (1984) 1272.
23. K.-H. Schmidt, C.-C. Sahm, K. Pielenz, and H.-G. Clerc, *Z. Phys.* **A316** (1984) 19.
24. G. Audi, O. Bersillon, J. Blachot, and A. H. Wapstra, *Nucl. Phys.* **A624** (1997) 1.
25. R. B. Firestone, V. S. Shirley, C. M. Baglin, S. Y. F. Chu, and J. Ziplin, *Table of Isotopes* (John Wiley and Sons, 1996).
26. W. M. Howard and P. Möller, *At. Data and Nucl. Data Tables* **25** (1980) 219.
27. W. Nazarewicz, *Phys. Lett.* **B305** (1993) 195.
28. S. Ćwiok, W. Nazarewicz, J. X. Saladin, W. Plóciennik, and A. Johnson, *Phys. Lett.* **B322** (1994) 304.
29. D. Kolb and A. Marinov, *Proc. Int. Conf. Nucl. Phys.*, Florence, Vol. 1 (1983) p. 92.
30. A. Marinov, S. Eshhar, J. L. Weil, and D. Kolb, *Phys. Rev. Lett.* **52** (1984) 2209; **53** (1984) 1120(E).
31. A. Marinov, S. Gelberg and D. Kolb, *6th Int. Conf. on Nuclei Far from Stability and 9th Int. Conf. on Atomic Masses and Fundamental Constants*, Bernkastel-Kues, Germany, *Inst. Phys. Conf. Ser.* No. 132 (1992) p. 437.
32. K. Kumar, *Superheavy Elements* (Adam Hilger, Bristol and New York, 1989).
33. J. P. Blocki, H. Feldmeier and W. J. Swiatecki, *Nucl. Phys.* **A459** (1986) 145.